

# The Effect of pH and Metal Loading on the Properties of Sol–Gel Rh/SiO<sub>2</sub>

Christine K. Lambert and Richard D. Gonzalez<sup>1</sup>

*Department of Chemical Engineering, Tulane University, New Orleans, Louisiana 70118*

Received July 17, 2000; in revised form December 7, 2000; accepted January 19, 2001; published online March 26, 2001

Rh/SiO<sub>2</sub>, to be used as a potential catalytic material, was prepared using sol–gel processing. Tetraethoxysilane (TEOS) was used as the support precursor and Rh(acac)<sub>3</sub> was used as the metal precursor. Nitrogen full-sorption was used to determine surface area, average pore size, and total pore volume of the support, while hydrogen chemisorption and electron microscopy were used to determine metal particle size. Samples prepared at a pH of about 3 had a high metal dispersion and well-defined pore size distribution. Designed metal loading was varied from 0.5 to 1.5 wt%. Dried gels were probed using <sup>29</sup>Si Solid state MAS NMR, and the relative amount of partially and fully condensed (Q<sub>2</sub>, Q<sub>3</sub>, Q<sub>4</sub>) silicon centers was quantified. As the metal loading was increased, the gels became more fully condensed. Silica prepared at a pH of about 8 showed a significant increase in the degree of condensation regardless of the rhodium content. © 2001 Academic Press

## 1. INTRODUCTION

The preparation of supported metal catalysts by sol–gel processing is an interesting area of research. The method is unique because the metal precursor is mixed homogeneously together with the molecular precursor of the support, resulting in a greater degree of control over the final properties of the catalyst. The support precursor is usually a metal alcoxide that can be hydrolyzed and then condensed to form a gel network. By the variation of several preparative conditions, one can tailor-make a support with the desired properties for a particular application. These variables include pH, water/metal alcoxide ratio (*R*), gelation temperature, metal loading, addition of dopants, solvent removal, and pretreatment conditions. Silica xerogels are easily prepared from tetraethoxysilane (TEOS) under acidic or basic conditions leading to supports with well-defined pore size distributions and high surface areas.

The ability to control the pore size of silica through sol–gel processing has led to the preparation of thermally resistant catalysts such as Pd/SiO<sub>2</sub>, (1), PtSiO<sub>2</sub> (2, 3), and

Rh/SiO<sub>2</sub> (4). The goal of these studies was to match the metal particle size of the reduced catalyst to the pore size of the support. This was accomplished by manipulating a few of the preparative variables. The size match led to a decrease in deactivation by sintering when compared to traditional catalysts prepared by ion-exchanging noble metal salts onto commercial supports. The improved thermal stability was attributed to the decreased diffusion of the supported metal particles within the mesoporous support (5). Noble metal acetylacetonate compounds [Pd(acac)<sub>2</sub>, Pt(acac)<sub>2</sub>, and Rh(acac)<sub>3</sub>] were used as metal precursors due to their high solubility in acetone. This allowed the precursor to be added to the initial sol–gel mixture of TEOS, ethanol, and water. No attempt was made to cause an interaction between the metal precursor and the support except for constant mixing to establish homogeneity in the final gel.

Other researchers have prepared silica-supported noble metal catalysts by the sol–gel method with the intention of anchoring the noble metal precursor onto the support. This is accomplished by either altering the support precursor or the metal precursor to include a reactive moiety. For example, triethoxysilane has been mixed with Pd(OAc)<sub>2</sub> in an aqueous/organic solution to prepare a Pd/SiO<sub>2</sub> catalyst (6), and X(CH<sub>2</sub>)<sub>3</sub>Si(OEt)<sub>3</sub>, where X = NH<sub>2</sub>, NHCH<sub>2</sub>CH<sub>2</sub>NH<sub>2</sub> or CN has been reacted with several metal compounds including Pd(acac)<sub>2</sub> and Pt(acac)<sub>2</sub> (7). In another study, Pd<sup>2+</sup> [(NH<sub>2</sub>–CH<sub>2</sub>–CH<sub>2</sub>–NH–(CH<sub>2</sub>)<sub>3</sub>–Si(OCH<sub>3</sub>)<sub>2</sub>)<sub>2</sub> was cogelled with tetraethoxysilane (8). A common feature of these studies was the high dispersion of the final catalyst.

In this paper, the effect of pH on the preparation of silica supports from TEOS is investigated; the use of acetone as a solvent in the sol–gel mixture is also investigated. The addition of acetone is necessary in the preparation of Rh/SiO<sub>2</sub> in order to completely dissolve the metal precursor. The effect of pH and metal loading on the surface area, average pore diameter, pore volume, and dispersion of Rh/SiO<sub>2</sub> catalysts is reported. Actual metal loadings are reported as measured by ICP analysis at Galbraith Laboratories in Knoxville, TN. Deconvolution data from <sup>29</sup>Si solid state NMR spectra are used to show the effect of pH, solvent, and metal loading on the silica gel structure.

<sup>1</sup>To whom correspondence should be addressed. E-mail: gonzo@mail-host.tcs.tulane.edu.

## 2. EXPERIMENTAL

### 2.1. Preparation of Rh/SiO<sub>2</sub> Catalysts

The catalyst precursors were tetraethoxysilane (TEOS) and Rh (III) 2,4-pentanedionate (Alfa Aesar, Ward Hill, MA). The metal precursor is also known as rhodium acetylacetonate, or Rh(acac)<sub>3</sub>. This compound was chosen because of its high solubility in acetone and simple decomposition at a moderate temperature (280°C). In a typical synthesis, 15 ml of TEOS was dissolved in 10 ml of ethanol and heated at 45°C. A designed amount of Rh(acac)<sub>3</sub> was dissolved in 10 ml of acetone and also heated to 45°C. The two solutions were thoroughly mixed together and deionized water was added in an amount in excess of that required for stoichiometry ( $R = \text{mol H}_2\text{O}/\text{mol TEOS} \sim 10$ ). The pH was sometimes manipulated through the addition of HCl or NH<sub>4</sub>OH. The resulting homogeneous yellow solution was stirred continuously in a rotary evaporator at 50°C until gelation. Following the formation of a gel, the temperature was increased to 80°C for a period of approximately 1 h. The purpose of this heat treatment was to evaporate the ethanol and acetone prior to the drying step (4). This ensured the formation of a xerogel with a narrow pore size rather than an aerogel. Final drying was performed in an oven at 110°C for a period of 16 h.

### 2.2. Preparation of Blank Silica

Blank SiO<sub>2</sub> xerogels were prepared by sol-gel processing. TEOS was dissolved in ethanol and heated to 45°C, and sometimes acetone was used as an additional solvent. The amount of acetone added was 10 ml, which was the same amount as for samples containing Rh. A designed amount of deionized water in excess of stoichiometry was added. Either HCl or NH<sub>4</sub>OH were used to manipulate the pH of the solution, which was then placed in a rotary evaporator at 50°C and constantly stirred until gelation. The temperature was raised to 80°C for approximately 1 h. The gel was dried at 110°C for 16 h to form a xerogel.

### 2.3. Thermal Analysis

Thermogravimetric analysis (TGA) was performed on the dried gels with a Hi-Res TGA 2950 Thermogravimetric Analyzer from TA Instruments. The analysis was performed in flowing O<sub>2</sub> at 100 ml min<sup>-1</sup> temperature ramp. A Thermolab mass spectrometer, in series with the TGA, was used to determine the identity of the gases evolved from the sample.

### 2.4. Pretreatment Procedure

Prior to any further characterization studies, about 200 mg of sample was placed in a pyrex microreactor. The

sample was heated in flowing O<sub>2</sub> at a rate of 10°C min<sup>-1</sup> to a final temperature of 400°C and held at this temperature for 30 min. The Rh/SiO<sub>2</sub> catalysts were also reduced in flowing H<sub>2</sub> at 400°C for 1 h. Argon was used to flush out the reactor between O<sub>2</sub> and H<sub>2</sub> treatments. The pretreatment temperature was maintained using a temperature programmer and a gas flow rate of 30 ml min<sup>-1</sup> was obtained using Tylan mass flow controllers. All gases were UHP grade and the appropriate heaters and traps were used to maintain the integrity of the gas streams.

### 2.5. Surface Area and Pore Size Measurements

A Coulter Omnisorb Porosimeter was used to measure the surface area and pore size distribution of all the materials prepared. A 100-mg sample was placed in a pyrex holder, heated to 200°C, and evacuated to 10<sup>-5</sup> torr. The full adsorption-desorption isotherm was obtained at 77 K using UHP nitrogen. Surface areas were calculated using the BET equation, and pore size distributions were obtained from the desorption isotherm. For microporous gels (pore diameter < 2 nm), the Langmuir surface area was calculated, and the average pore size was approximated by the Harkins-Jura equation using the adsorption isotherm.

### 2.6. Hydrogen Chemisorption

Hydrogen chemisorption measurements were performed using the dynamic pulse method. This procedure has been described in detail elsewhere (9). Weakly adsorbed hydrogen is not measured when this method is used. Approximately 200 mg of catalyst was placed in a pyrex microreactor and subjected to the standard pretreatment at 400°C. The reactor was flushed with argon and rapidly cooled at 25°C. Small amounts of H<sub>2</sub> (85.8 μl) were pulsed through the reactor until saturation was attained. A gas chromatograph equipped with a thermal conductivity detector was used to monitor the volume of H<sub>2</sub> leaving the reactor following the addition of each pulse. The saturation point was determined when the integrated area from successive eluted peaks was equal.

### 2.7. Solid State NMR

A Bruker DX300 solid state NMR was used to determine the extent of condensation in the dried gels. <sup>29</sup>Si MAS spectra were taken at 59.6 MHz using a 4-mm rotor at a rotating speed of 14 kHz. A 7-mm rotor was also used at a rotating speed of 6.5 kHz. A 2-μs high power pulse was used with a 30-s time delay between pulses and 2000 scans were taken for each peak. The Q<sub>n</sub> nomenclature was used to denote the number of Si-O-Si bonds present about a silicon center. Up to three distinct peaks were found for each sample corresponding to the Q<sub>2</sub>, Q<sub>3</sub>, and Q<sub>4</sub> species. The

spectra for a sample of sol-gel silica dried at 110°C or calcined at 400°C were identical.

### 2.8. Electron Microscopy

A Phillips EM 410-transmission electron microscope equipped with a LaB<sub>6</sub> filament was used to determine metal particle size distributions. The samples were prepared by sonicating 10 mg of catalyst in 30 ml of ethanol. One drop of the suspension was placed on a holey carbon copper grid and allowed to dry completely. Typical magnifications required were 184,000 with an accelerating voltage of 80 keV. Photographs were enlarged to 8" × 10" size to allow

**TABLE 1**  
Effect of pH on the Structure of Sol-Gel Silica

pH	BET area (m <sup>2</sup> /g)	Pore vol. (ml/g)	Avg. pore. diameter				
			Q <sub>2</sub> (%)	Q <sub>3</sub> (%)	Q <sub>4</sub> (%)	Q <sub>4</sub> /Q <sub>3</sub>	
1	524 <sup>a</sup>	0.20	0.6	2.2	51.8	46.1	0.9
3	502	0.23	3.4	1.0	45.2	53.9	1.2
8	174	0.53	6, 18	0	15.3	84.7	5.6

<sup>a</sup>Langmuir surface area.

measurement of particle size with a micrometer. Approximately 10 spots from photographs of each sample were analyzed to obtain size distributions.

## 3. RESULTS

### 3.1. Effect of pH on Blank SiO<sub>2</sub> Gels

The effect of pH on the structural properties of the calcined SiO<sub>2</sub> gels is most apparent from the full-sorption isotherms shown in Fig. 1. The isotherm for the sample prepared at a pH of 1 is microporous (Type I), while the isotherm for the sample prepared at a pH of 8 is clearly mesoporous (Type IV). The physical properties of the gels are shown in Table 1. Surface area decreases as the pH is increased, while the pore volume and average pore diameter are observed to increase. The solid state NMR data shows a decrease in Q<sub>2</sub> and Q<sub>3</sub> species and an increase in Q<sub>4</sub> species. In the last column, the ratio of Q<sub>4</sub>/Q<sub>3</sub> species is shown, indicating the relative extent of condensation. The gel becomes significantly more condensed with increasing pH. The spectra are shown in Fig. 2 for comparison.

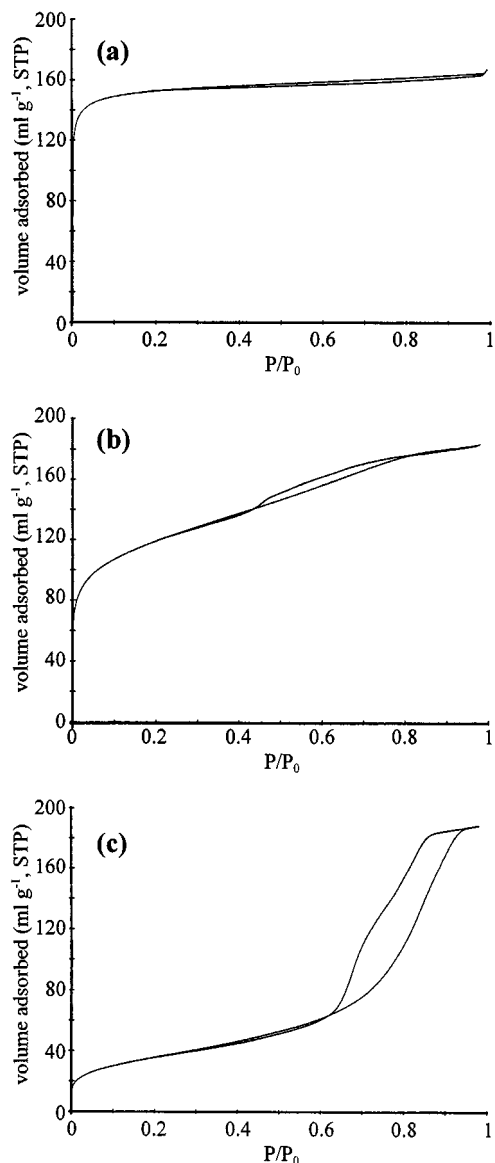


**FIG. 1.** Nitrogen full-sorption isotherm at 77 K for SiO<sub>2</sub> prepared at (a)  $R = 4$ , pH 1; (b)  $R = 10$ , pH 3; (c)  $R = 10$ , pH 8.

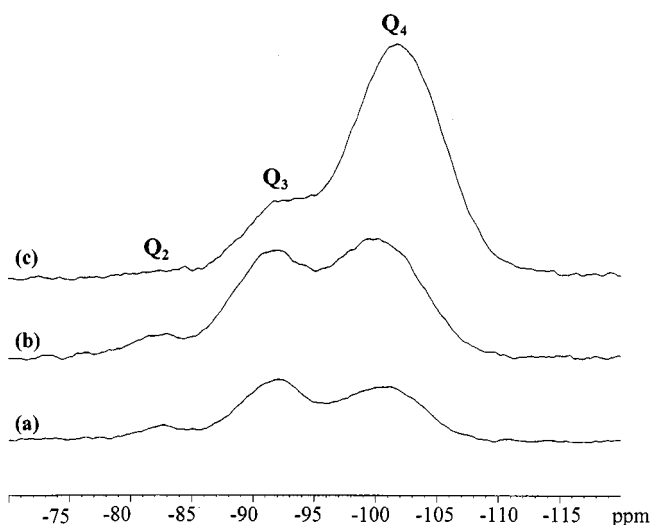


**FIG. 2.** <sup>29</sup>Si solid state NMR spectra for blank SiO<sub>2</sub> prepared at (a)  $R = 4$ , pH 1.0; (b)  $R = 10$ , pH 3; (c)  $R = 10$ , pH 8.

**TABLE 2**  
The Structure of Sol-Gel Silica Prepared with Acetone

R	pH	Langmuir area (m <sup>2</sup> /g)	Pore vol. (ml/g)	Avg. Pore diameter (nm)	Q <sub>2</sub> (%)	Q <sub>3</sub> (%)	Q <sub>4</sub> (%)	Q <sub>4</sub> /Q <sub>3</sub>
10	3	697	0.28	0.6	2.5	47.7	49.8	1.1
30	3	829	0.34	0.5	1.9	50.6	47.5	0.9

### 3.2. Effect of Solvent on Blank SiO<sub>2</sub>

The effect of adding 10 ml of acetone to the TEOS/ethanol/H<sub>2</sub>O mixture was studied at a pH of 3 and an R ratio of 10 and 30. The physical properties of the calcined gels are shown in Table 2. The samples have high surface areas and microporous structures. The addition of acetone results in a further branching of the silica structure as evidenced by the decreasing Q<sub>4</sub>/Q<sub>3</sub> ratio. This is probably due to the further dilution of the silica precursor when additional solvent is added. Also acetone, a fairly polar solvent, may decelerate the condensation rate through stabilization of the negatively charged reactants ( $\equiv \text{SiO}^{-1}$ ) (10, 11), although the small amount used here does not cause a significant effect.

### 3.3. Effect of pH on Rh/SiO<sub>2</sub>

The effect of pH on the structure of Rh/SiO<sub>2</sub> is similar to the effect on blank SiO<sub>2</sub>. The physical properties of the pretreated catalysts are shown in Table 3. At a pH of about 2, the resulting gel is microporous with a high surface area, low pore volume, and moderate dispersion. At a pH between 2 and 4, the surface area decreases, the pore volume increases, and the dispersion reaches a maximum value at a pH of 3.6. The average pore diameter in this pH range is mesoporous with a well-defined pore size distribution. At pH > 8 the gel has a broad pore size distribution and low metal dispersion. The Q<sub>4</sub>/Q<sub>3</sub> ratio increases with increasing pH, indicating a more fully condensed silica structure. The <sup>29</sup>Si NMR spectra are shown in Fig. 3 for comparison. The

actual metal loading for all of the catalysts are lower than the designed metal loading of 1 wt%, and the actual metal loading increases with increasing pH.

The weight loss curves resulting from the heating of the dried Rh(acac)<sub>3</sub>/SiO<sub>2</sub> gels in an oxygen atmosphere are shown in Fig. 4. Also shown are the first derivative curves. The initial weight loss has been identified as physisorbed water, while weight loss at 280°C consists of CO<sub>2</sub> and H<sub>2</sub>O and is due to the decomposition of the supported Rh(acac)<sub>3</sub>. The samples exhibit similar weight transitions with the exception of the sample prepared at a pH of 8.8. The decomposition of Rh(acac)<sub>3</sub> in this sample is very sharp and occurs at a slightly lower temperature than that for the other three samples.

### 3.4. Effect of Metal Loading

The physical properties of the Rh/SiO<sub>2</sub> catalysts prepared with designed metal loadings of 0.5, 1.0, and 1.5 wt% at a pH of approximately 3 are shown in Table 4. Thermal analysis of the dried gels results in similar decomposition curves as shown in Fig. 5. The only significant difference is the magnitude of the second weight loss, which increases with increased metal loading as expected. The actual metal loadings are lower than the designed values, and this often occurs in samples that have been prepared by the sol-gel method as discussed in a previous paper (16). As the metal loading increases, the BET surface area decreases while the pore volume and average pore diameters remain almost constant. The extent of condensation (Q<sub>4</sub>/Q<sub>3</sub>) increases with increased metal loading, as shown in Table 5. The increase

**TABLE 3**  
Effect of pH on the Physical Properties of Sol-Gel Rh/SiO<sub>2</sub> (1 wt% Designed Metal Loading)

Sample	pH	Rh (wt %)	BET area (m <sup>2</sup> /g)	Pore vol. (ml/g)	Avg. pore diameter (nm)	D <sub>H</sub> <sup>b</sup> (%)	Q <sub>4</sub> /Q <sub>3</sub>
RS1	0.5	0.50	298 <sup>a</sup>	0.13	0.7	37	1.5
RS2	2.8	0.60	702	0.13	3.2	39	1.8
RS3	3.6	0.74	590	0.44	3.8, 6	60	1.9
RS4	8.8	0.95	281	0.45	18.0	27	5.1

<sup>a</sup>Langmuir surface area.

<sup>b</sup>D<sub>H</sub> = dispersion as measure by H<sub>2</sub> chemisorption.

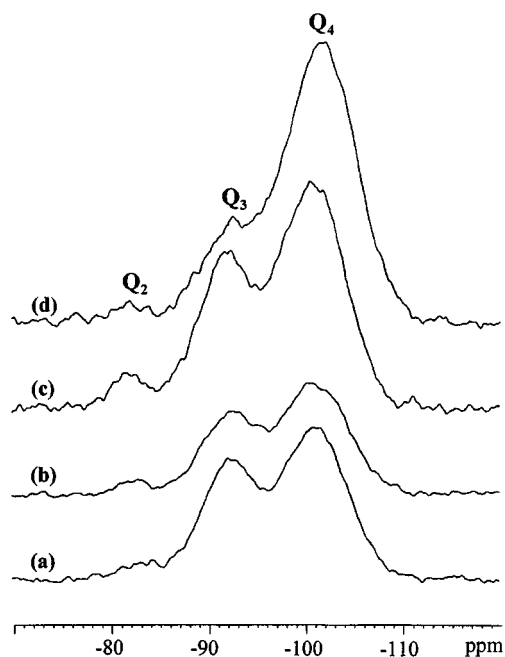


FIG. 3.  $^{29}\text{Si}$  solid state NMR spectra for Rh/SiO<sub>2</sub> prepared at  $R = 10$  and (a) pH 0.5, (b) pH 2.8, (c) pH 3.6, and (d) pH 8.8.

in condensation of the support is further illustrated in Fig. 6, which shows the pore size distribution of the Rh/SiO<sub>2</sub> samples. There are clearly more pores present in the 0.4 wt% Rh sample, and the number of pores decreases with increasing metal loading. Metal particle sizes are estimated from hydrogen chemisorption data and TEM measurements. A stoichiometry for of 1:1 for Rh<sub>(surf)</sub>:H and 7.6 Å<sup>2</sup> per surface metal atom (12) was assumed. The average metal particle size calculated from chemisorption and TEM do not agree exactly, but the trend in size vs metal loading is the same.

The rhodium particle size distributions from TEM are shown in Fig. 7. Most of the particles are between 3 and 5 nm with particles ranging up to 17 nm in the most heavily loaded sample. Example micrographs of these three samples are shown in Fig. 8.

TABLE 4  
Effect of Metal Loading on the Physical Properties of Sol-Gel Rh/SiO<sub>2</sub>

Sample	Des. Rh wt%	ICP Rh wt%	pH	BET area (m <sup>2</sup> /g)	Pore vol. (ml/g)	Avg. pore diameter (nm)	$D_H$ (%)	$D_H^b$	$d_m^a$ (nm)	TEM
RS5	0.5	0.41	3.2	601	0.49	3.8, 5	45	2.0	3.8	
RS3	1.0	0.74	3.6	590	0.44	3.8, 6	60	1.5	1.7	
RS6	1.5	0.89	2.9	482	0.50	3.8, 10	12	7.6	6.7	

<sup>a</sup> $d_m$  = metal particle size.

<sup>b</sup> $d_m$  calculated from  $D_H$  assuming a 1:1 stoichiometry for Rh<sub>(surf)</sub>:H and 7.6 Å<sup>2</sup> per surface metal atom (12).

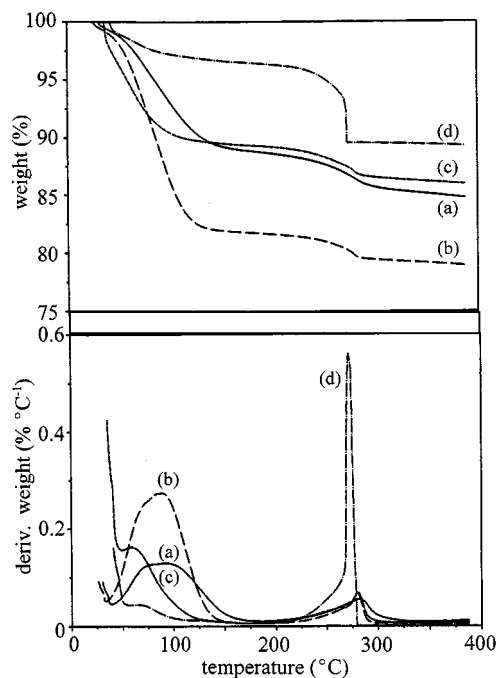
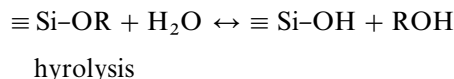


FIG. 4. Thermogravimetric weight loss and first derivative weight loss curves for dried Rh/SiO<sub>2</sub> gels in an oxygen atmosphere: (a) pH 0.5, (b) pH 2.8, (c) pH 3.6, and (d) pH 8.8.

#### 4. DISCUSSION

In the presence of excess water, the pH of the sol-gel solution is the most important variable in determining the final structure of silica gel. The effect of pH on the formation of SiO<sub>2</sub> from TEOS has been extensively studied (13–15). There are three reaction regimes depending upon the pH of the sol: pH < 2, 2 < pH < 7, and pH > 7. In general, the sol-gel reactions are:



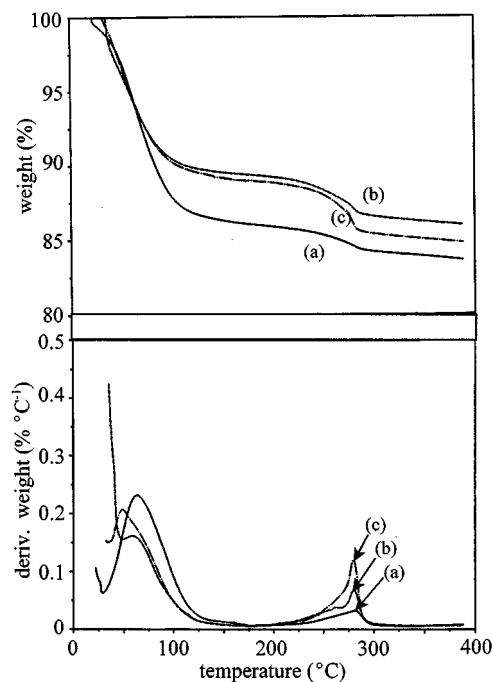
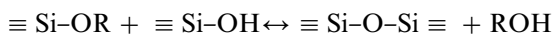
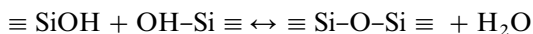


FIG. 5. Thermogravimetric weight loss and first derivative weight loss curves for dried Rh/SiO<sub>2</sub> gels in oxygen atmosphere: (a) 0.41 wt% Rh, (b) 0.74 wt% Rh, (c) 0.89 wt% Rh.



alcohol condensation



water condensation

At a pH < 2, the rate of reaction is proportional to [H<sup>+</sup>]. At a pH of 2–7, the condensation rate is also relative to the hydrolysis rate and is proportional to [OH<sup>-</sup>]. Above a pH of 7, the reaction mechanism is the same as for a pH of 2–7, but the mechanism of particle growth is different. Instead of forming a network by particle aggregation, the particles are more highly condensed and grow through the addition of

TABLE 5  
<sup>29</sup>Si Solid State NMR for Rh/SiO<sub>2</sub> Gels Prepared with Different Designed Metal Loadings (R=10, pH ~ 3)

Sample	Des. Rh wt%	Q <sub>2</sub> (%)	Q <sub>3</sub> (%)	Q <sub>4</sub> (%)	Q <sub>4</sub> /Q <sub>3</sub>
SiO <sub>2</sub>	0	2.5	47.7	49.8	1.1
SiO <sub>2</sub> <sup>a</sup>	0	1.0	45.2	53.9	1.2
RS5	0.5	0.5	38.6	60.9	1.6
RS3	1.0	1.3	34.0	64.7	1.9
RS6	1.5	1.3	29.2	69.6	2.4

<sup>a</sup>Prepared without acetone.

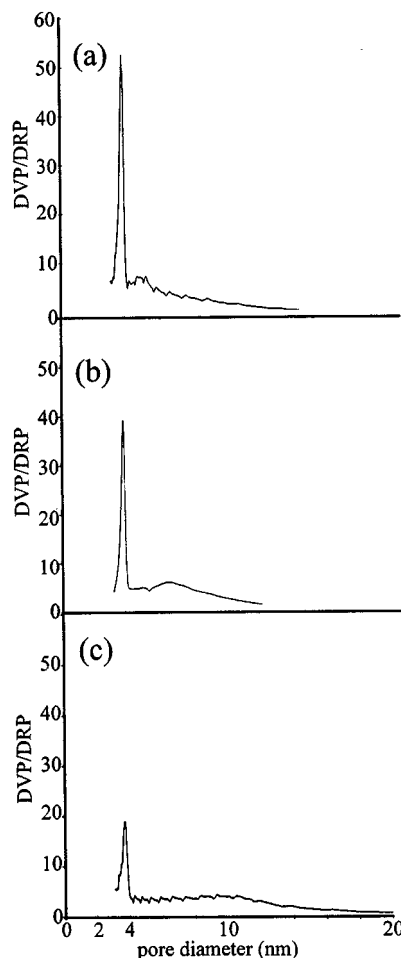


FIG. 6. Pore size distributions for Rh/SiO<sub>2</sub> catalysts prepared at R = 10 and pH 3: (a) 0.41 wt% Rh, (b) 0.74 wt% Rh, (c) 0.89 wt% Rh.

monomers. This results in lower surface areas and larger pores than for gels obtained from the other two regimes. The results for the silica gels prepared in this study at different values of pH support the three-regime theory as evidenced by the final physical properties of the gels and <sup>29</sup>Si NMR spectra of the gel structure.

The support structure of the silica with supported Rh is affected by pH in a similar way. The sample prepared at a pH value of about 3.6 has a mesoporous structure that is capable of stabilizing the dispersion of the supported metal at temperatures up to 650°C (4). This is due to the physical size match between the pore diameter and the particle size of Rh. Other workers (1, 2) have found that the preparation of sol-gel catalysts at a pH of 3–5 results in similar mesoporosity, metal dispersion, and increased thermal stability.

The actual metal loading of the catalysts as measured by ICP analysis is always less than the designed value. This is typical for sol-gel catalysts prepared with acetylacetonates (16). The sublimation temperature of Rh(acac)<sub>3</sub> is 240°C

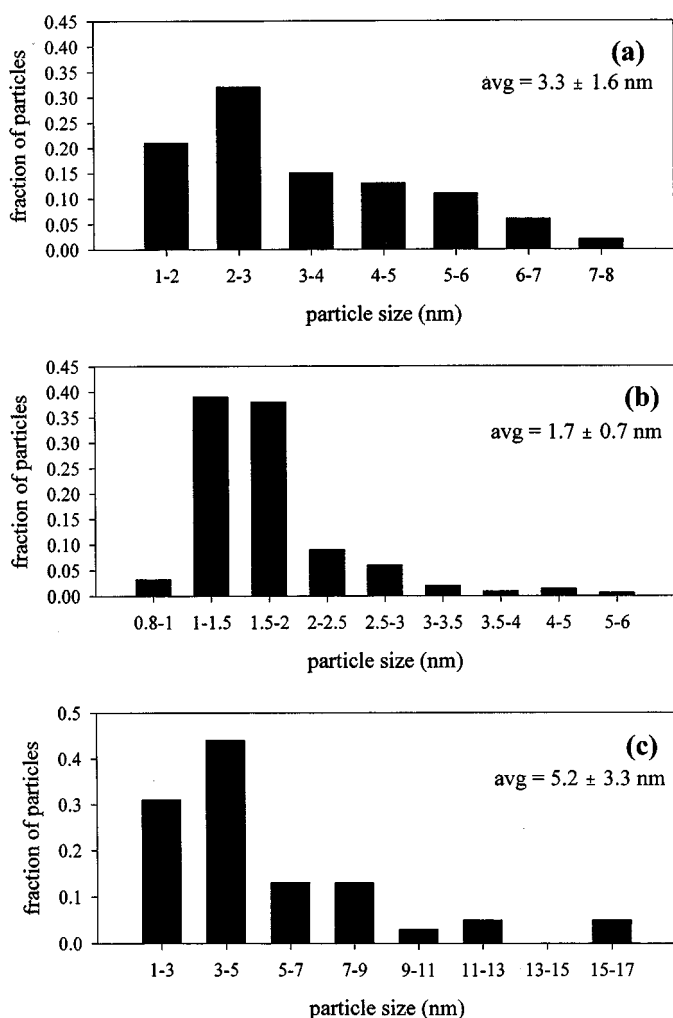


FIG. 7. Particle size distributions obtained from TEM for Rh/SiO<sub>2</sub> catalysts prepared at  $R = 10$  and pH 3: (a) 0.41 wt% Rh, (b) 0.74 wt% Rh, (c) 0.89 wt% Rh.

while its decomposition temperature is 280°C. This effect results in some metal loss as evidenced by a Rh mirror that was formed downstream of the microreactor after several catalyst pretreatment steps.

The addition of acetone, a necessary step in the preparation of the Rh/SiO<sub>2</sub> by sol-gel, has a much more subtle effect on the support structure in that it decreases the extent of the condensation reaction through dilution and stabilization of intermediate silicate species. The addition of Rh(acac)<sub>3</sub> has the opposite effect. From the thermal analysis data, it is apparent that Rh(acac)<sub>3</sub> remains intact throughout the sol-gel reactions and does not decompose until the catalyst is calcined at 280°C. Increasing the amount of the metal precursor while maintaining a constant pH increases the extent of condensation. Therefore, Rh(acac)<sub>3</sub> is acting as a catalyst which promotes the condensation reaction. A similar catalytic effect has been noted by Zhang *et al* (17). In the

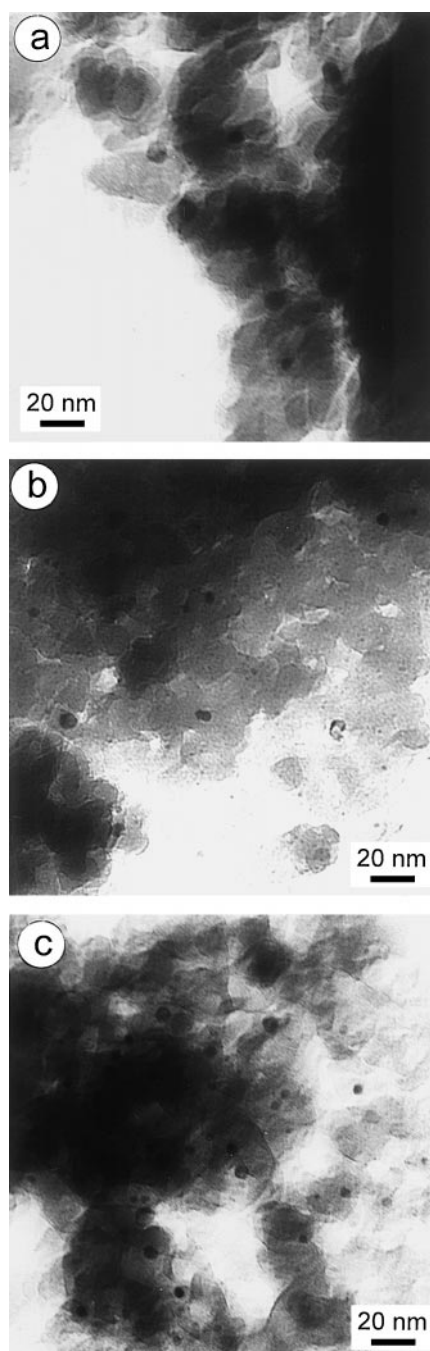


FIG. 8. TEM micrographs of Rh/SiO<sub>2</sub> catalysts prepared at  $R = 10$  and pH 3: (a) 0.41 wt% Rh, (b) 0.74 wt% Rh, (c) 0.89 wt% Rh. The magnification used was 185 k and enlarged by a factor of 2.7.

preparation of CH<sub>3</sub>SiO<sub>3/2</sub> gels from methyltriethoxysilane, infrared suggested that the presence of Al(acac)<sub>3</sub> in the sol-gel mixture caused the formation of more stable linear products and further polymerization of the precursor. The mechanism by which the acetylacetonate does this is not clear, but other workers have noted that Zn(acac)<sub>2</sub> can act

as a templating agent in the formation of aluminosilicates by sol-gel, resulting in mesoporous materials (18). This was explained by a complexation between the compound and aluminum through keto-enol tautomerization. Rh(acac)<sub>3</sub> does not react chemically with metal oxide surfaces and is only physisorbed in organic media (19, 20). In a study of the degree of hydration of metal acetylacetonates, the distribution of the compounds between water and CCl<sub>4</sub> was measured (21). Rh(acac)<sub>3</sub> was the least hydrated compound because of its high electron density. Another study found that some tri-acetylacetonates are capable of hydrogen bonding to water and methanol (22). Rh(acac)<sub>3</sub> is capable of complexation with silicate intermediates and catalyzing the condensation reaction.

## 5. CONCLUSIONS

In this study, the effect of pH and metal loading on the properties of Rh/SiO<sub>2</sub> catalysts by sol-gel processing was presented. The pH of the sol had the most significant effect on the final silica support structure. A secondary effect of solvent, in this case acetone, was a result of dilution and polarity effects. The preparation of Rh/SiO<sub>2</sub> at a pH of about 3 with excess water results in a mesoporous material with a well-defined pore size distribution and high metal dispersion. An increase in metal loading at constant pH increases the degree of condensation of the silica support due to a catalytic effect of Rh(acac)<sub>3</sub> on the sol-gel polymerization reactions.

## ACKNOWLEDGMENTS

The authors acknowledge the U.S. Department of Energy (DOEFGO2-86ER-1351), the Louisiana Board of Regents (LEQSF-ENG-TR-49), and

the National Science Foundation for their support. We also thank the Electron Microscopy Laboratories at the Louisiana State University School of Veterinary Medicine and Tulane University for the use of their facilities.

## REFERENCES

1. W. Zou and R. D. Gonzalez, *Appl. Catal. A: Gen.* **126**, 351 (1995).
2. W. Zou and R. C. Gonzalez, *Appl. Catal. A: Gen.* **102**, 181 (1993).
3. W. Zou and R. D. Gonzalez, *J. Catal.* **152**, 291 (1995).
4. C. K. Lambert and R. D. Gonzalez, *Microporous Mater.* **12**, 179 (1997).
5. E. Ruckenstein and B. Pulvermacher, *J. Catal.* **37**, 416 (1975).
6. J. M. Tour, S. L. Pendelwar, and J. P. Cooper, *Chem. Mater.* **2**, 647 (1990).
7. B. Breitscheidal, J. Zeider, and U. Schubert, *Chem. Mater.* **3**, 559 (1991).
8. B. Heinrichs, F. Noville, and J.-P. Pirard, *J. Catal.* **170**, 366 (1997).
9. J. Sarkany and R. D. Gonzalez, *J. Catal.* **76**, 75 (1982).
10. I. Artaki, T. W. Zerda, and J. Jonas, *J. Non-Cryst. Solids* **81**, 381 (1986).
11. K. Chou and B. I. Lee, *J. Mat. Sci.* **29**, 3565 (1994).
12. D. J. C. Yates and J. H. Sinfelt, *J. Catal.* **8**, 348 (1967).
13. R. Aelion, A. Loebel, and F. Eirich, *J. Am. Chem. Soc.* **72**, 5705 (1950).
14. R. K. Iler, "The Chemistry of Silica," Wiley, New York, 1979.
15. C. J. Brinker and G. W. Scherer, "Sol-Gel Science: The Physics and Chemistry of Sol-Gel Processing," Academic Press, San Diego, 1990.
16. C. K. Lambert and R. D. Gonzalez, *Appl. Catal. A: Gen.* **172**, 233 (1998).
17. Z. Zhang, Y. Tanigami, and R. Terai, *J. Non-Cryst. Solids* **191**, 304 (1995).
18. J. M. Miller, D. Wails, J. S. Hartman, and J. L. Belelie, *J. Chem. Soc. Faraday Trans.* **94**, 789 (1998).
19. J. A. Rob van Veen, G. Jonkers, and W. H. Hesselink, *J. Chem. Soc. Faraday Trans.* **1**, 389 (1989).
20. N. K. Raman, T. L. Ward, C. J. Brinker, R. Sehgal, D. M. Smith, Z. Duan, M. Hampden-Smith, J. K. Bailey, and T. J. Headly, *Appl. Catal. A: Gen.* **69**, 65 (1993).
21. P. D. Hopkins and B. E. Douglas, *Inorg. Chem.* **3**, 357 (1966).
22. T. S. Davis and J. P. Fackler, *Inorg. Chem.* **5**, 242 (1966).